Early response assessment in prostate carcinoma by ¹⁸F-fluorothymidine following anticancer therapy with docetaxel using preclinical tumour models

**Nobuyuki Oyama · Yoko Hasegawa · Yasushi Kiyono · Masato Kobayashi ·
Yasuhisa Fujibayashi · Datta E. Ponde · Carmen Dence · Michael J. Welch ·
Osamu Yokoyama**

Abstract

Purpose The aim of the study was to assess the potential usefulness of 3-deoxy-3-¹⁸F-fluorothymidine (FLT) as a radiopharmaceutical for imaging the early therapeutic effects of docetaxel (DTX) on tumour proliferation in hormone-refractory prostate cancer (HRPC).

Methods Cells of the androgen-independent human prostate tumour cell line, 22Rv1, were implanted in athymic male mice. Approximately 3 weeks after cell implantation, the mice were treated with DTX or vehicle. Before and after the treatment, the mice were imaged with a microPET-Focus-F120 scanner (Concorde Microsystems, Knoxville, TN, USA) using FLT and ¹⁸F-fluorodeoxyglucose (FDG). Tracer accumulations in the tumours were then analysed and compared with the proliferation activity and apoptotic index of the tumours. In a separate cell study, 22Rv1 cells were treated with DTX, then incubated with FLT or FDG and examined for their tracer uptake.

Results The microPET imaging showed a significant decrease of FLT uptake in tumours after administration of DTX, while the changes of FDG uptake were minimal. Immunohistochemical analysis of the tumours revealed that the changes of FLT uptake were well correlated with those of proliferation activity but not with the apoptotic index. In vitro studies demonstrated that the significant decrease of FLT uptake in the cells after incubation with DTX correlated with the % S-phase cell fraction, while there were only minimal changes in the prostate-specific antigen concentration of the cell medium and FDG uptake in the cells.

Conclusion These results indicate that FLT is a promising tracer for monitoring the early effects of anticancer therapy with DTX in patients with HRPC.

Keywords PET · Prostate cancer · Docetaxel · Tumour proliferation · ¹⁸F-Fluorothymidine

N. Oyama (✉) · Y. Hasegawa · O. Yokoyama
Department of Urology, Faculty of Medical Sciences,
University of Fukui,
23-3 Matsuoka-Shimoaizuki,
Fukui 9101193, Japan
e-mail: urono@u-fukui.ac.jp

Y. Kiyono · M. Kobayashi · Y. Fujibayashi
Biomedical Imaging Research Center, University of Fukui,
Fukui, Japan

D. E. Ponde · C. Dence · M. J. Welch
Mallinckrodt Institute of Radiology,
Washington University School of Medicine,
St. Louis, MO, USA

M. J. Welch
Siteman Cancer Center,
Washington University School of Medicine,
St. Louis, MO, USA

Introduction

Prostate cancer is the most commonly diagnosed cancer and is the second leading cause of cancer death in men over the age of 40 years in the USA [1]. Androgen dependency is a characteristic behaviour for most of the prostate cancers at first presentation [2]. Therefore, androgen ablation therapy (AAT) has been employed as the first-line treatment for patients with locally advanced disease or metastatic disease. Nonetheless, relapse after AAT remains a major problem. Many of the patients with hormone-refractory prostate cancer (HRPC) receiving AAT relapse within a few years of

treatment, and although chemotherapy is often considered one of the options for treating relapsed cancers, it is not as effective for prostate cancer as for other types of malignancy [3].

Recently, docetaxel (DTX)-based chemotherapy has been shown to improve survival in this disease [4]. After initiation of DTX therapy, conventional imaging modalities such as ultrasonography, computed tomography (CT) and magnetic resonance imaging (MRI) are employed to monitor the therapeutic effect by evaluating the anatomical changes of cancer lesions; however, the usefulness of these modalities is limited because they often require several months of treatment for the first accurate assessment. The anticancer effects of DTX can also be monitored by measuring the levels of serum prostate-specific antigen (PSA), but the reliability of this method is limited because HRPC tumours may have lost the ability to produce PSA or may produce less PSA than androgen-dependent prostate cancer tumours. Thus, there is a need for a more reliable diagnostic marker for the evaluation of the early therapeutic effect of DTX in patients with HRPC.

Positron emission tomography (PET) using the radiopharmaceutical 2-[^{18}F]fluoro-2-deoxy-D-glucose (FDG) has been widely accepted as a highly effective means for imaging a wide variety of cancers. FDG PET has been proven useful for monitoring the efficacy of prostate cancer treatments in both animal models [5] and humans [6, 7]. In these previous studies, treatment efficacy was monitored by using FDG PET to visualize metabolic changes of glucose in the prostate tumours following treatment. However, because the tumour grows relatively slowly in most cases, FDG PET has been previously shown not to be appropriate for initial diagnosis of primary as well as distant disease of prostate cancer [8, 9]. Urine excretion of this tracer is another disadvantage for imaging of prostate cancer and other urological malignancies.

Positron-labelled choline or acetate analogues have been reported to have higher sensitivity for the tumour detection of prostate cancer [10–12]. However, the usefulness of these tracers as cell proliferating markers of the tumours is limited [5, 13, 14], which may not be suitable for the evaluation of the early effect of anticancer therapy.

^{18}F-3′-Deoxy-3′-fluorothymidine (FLT) has been introduced as a radiopharmaceutical for use in assessing tumour proliferation by PET imaging [15]. Evaluation of the tumour proliferative activity by PET using FLT may have potential for assessing the viability of the tumour as well as the early effects of cancer therapy. In recent clinical studies, FLT uptake was higher in lung cancer tissue than in benign masses, indicating its usefulness for the differential diagnosis between malignant and benign tumours [16, 17]. Another previous study reported the use of FLT PET to evaluate breast cancer treatments [18]; the results indicated that FLT PET after the first course of chemotherapy was useful for predicting the long-term efficacy of chemotherapy regimens in women with breast cancer.

In our previous study, we demonstrated that FLT uptake in prostate tumours declined after initiation of AAT in an animal model and that this decline was correlated with the decrease of tumour size [5]. This was the first study which showed the possibility of using FLT PET imaging to monitor the therapeutic effects of AAT on prostate cancer.

The purposes of the present study were to determine whether microPET with FLT is useful for monitoring the early therapeutic effects of DTX in vitro and in vivo and also to determine whether FLT uptake in tumours correlates with the actual proliferative activity after DTX therapy.

Materials and methods

Radiochemical synthesis

FLT was synthesized as described previously. In brief, ^{18}F-fluoride was produced via the ^{18}O(p, n)^{18}F nuclear reaction by irradiating isotopically enriched ^{18}O-water with 15–16 MeV protons using either the Washington University Cyclotron Corporation CS-15 or the Japan Steel Works (JSW) BC-16/8 medical cyclotron. The radioactivity emerging from the target was resin treated to reclaim the ^{18}O-water. ^{18}F-Fluoride was eluted from the resin in a solution of 0.02 N potassium carbonate and used in subsequent reactions. FLT was synthesized starting with anhydrothymidine and microwave-mediated nucleophilic displacement by fluoride ion followed by acidic hydrolysis gave FLT in just 60 min [19]. The radiochemical yield was 12±4% (decay corrected) and the radiochemical purity was >99%.

Cellular uptake study

A well-established 22Rv1 human androgen-independent prostate adenocarcinoma cell line (American Type Culture Collection, Manassas, VA, USA) was chosen for our cellular uptake study. DTX was gifted by Sanofi-Aventis (Paris, France). Cells were maintained in RPMI 1460 medium (Gibco by Invitrogen, Carlsbad, CA, USA) containing 10% fetal bovine serum (FBS, Gibco by Invitrogen, Carlsbad, CA, USA) at 37°C in an atmosphere of 95% air and 5% CO_2. The cells were cultured in 24-well plates in quintuple at a concentration of $2×10^5$ cells per well. Forty-eight hours after incubation, when the cells reached 50% confluence in the wells, they were divided into three groups: group 1 was supplemented with 10% FBS medium, group 2 with 10% FBS medium with 10 nM DTX, and group 3 with 10% FBS medium with 100 nM DTX. After 24, 48 and 72 h of incubation with the respective media, 0.37 MBq of FLT or 0.37 MBq of FDG

was added to each well and the cells were further incubated for 2 h. After incubation with the tracers, 22Rv1 cells were harvested and the number of cells, % uptake of radioactivity into the cells, PSA concentration in the media and % S-phase fractions of cells in each group were determined.

Flow cytometric method

Immediately following the drug treatments described above, cells were harvested by trypsinization to obtain a single cell suspension. The cells were sedimented by centrifugation and treated with a CycleTEST™ PLUS DNA Reagent Kit (Becton Dickinson, San Jose, CA, USA) to prepare samples for DNA analysis on a flow cytometer, according to the manual from the manufacturer. The cell profiles of samples were analysed by flow cytometry (FACSCalibur, Becton Dickinson, San Jose, CA, USA). The resulting DNA histograms were analysed for determination of the % S-phase fraction using ModFit LT software (Becton Dickinson, San Jose, CA, USA).

MicroPET imaging

Animal experiments were conducted in compliance with the Guidelines for the Care and Use of Research Animals established by the Animal Studies Committee at our institution. Four- to six-week-old athymic nu/nu male mice were obtained from Charles River Laboratories (Wilmington, MA, USA). 22Rv1 cells have wild-type androgen receptors, grow in an androgen-independent fashion and produce PSA. Cells (2×10^5) were implanted subcutaneously into the right flank of the mice. Three weeks after tumour implantation, the mice were imaged in the prone position in a microPET-Focus-F120 scanner (Concorde Microsystems, Knoxville, TN, USA). For the baseline PET scans, mice were first anaesthetized with 1–2% isoflurane and placed in a prone position in a custom-designed holder that allows simultaneous imaging of two mice. The entire holder was placed near the centre field of view (CFOV) of the microPET scanner. The mice were injected intravenously with 7.7 MBq of ^{18}F-FLT and a 10-min static scan was obtained at 2 h post-^{18}F-FLT injection. A 10-min static scan was also obtained at 1 h post-^{18}F-FDG injection (7.7 MBq) on the next day. Following baseline PET imaging, six mice were treated with intravenous DTX (25 mg/kg) weekly for 2 weeks. Six control mice received no treatment. One week after the second DTX treatment, microPET imaging was repeated with the same protocol as described for the baseline studies. The methods of data collection and the reconstruction for microPET imaging have been described previously [5]. Briefly, all raw data were first sorted into three-dimensional (3-D) sinograms, followed by Fourier rebinning and 2-D filtered backprojection (FBP) reconstruction using a

ramp filter cutoff at the Nyquist frequency. A region of interest (ROI) was placed on each tumour or other organs in the transaxial microPET images that included the entire tumour or organ volume. The average radioactivity concentration within a tumour or an organ was obtained from the average pixel values within the multiple ROI volume. To eliminate the dependency on the injected total amount of radioactivity, tumour to muscle ratios were used to compare the FLT uptake in the tumour before and after the treatment. In these microPET scans, the attenuation corrections were not applied, since the accuracy of the measured attenuation correction was poor with this scanner, and since the amount of attenuation from the mouse body was relatively small and the shape of the mouse body did not change significantly among subjects; instead, the attenuation correction factors were incorporated into the system calibration. With the image reconstruction algorithm and filter described above, the resolution of this microPET system is between 2.0 and 3.0 mm full-width at half-maximum (FWHM) in each of the three dimensions within a 5-cm imaging FOV around the central axis of the tomograph. The partial volume effect in estimating the ROI values from microPET images is small in these studies, since the implanted tumours were more than 1 cm in diameter, which was well above the resolution limit of this system [20]. To assess the PSA production of implanted tumour, the serum PSA values of mice were also determined after the treatment.

Immunohistochemical examination of the 22Rv1 tumours

For histological evaluation of the degree of tumour proliferation and apoptosis, the tumours were excised, fixed in formalin, embedded in paraffin and cut into sections. Tumour sections were stained with mouse monoclonal antibodies for proliferating cell nuclear antigen (PCNA) (Dako, Carpinteria, CA, USA). PCNA labelling is an established measure of proliferation. PCNA is a 36,000 molecular weight, acidic, non-histone, nuclear protein in which the expression is associated with the late G and S phase of the cell cycle. A PCNA assay was performed on tumour slices, and proliferating cells were detected. Each experiment included three or four slices for each treatment. For each slice, a total of 100–200 nuclei were counted. For immunohistochemical detection of apoptosis, a TUNEL assay was performed using an ApopTag Peroxidase Kit (Intergen, Purchase, NY, USA). The TUNEL assay was performed on tumour slices obtained from mice after microPET scanning. Apoptotic nuclei were expressed as the percentage of the total nuclei counted. The tumour slices were fixed overnight in 10% neutral buffered formalin. After standard processing for the preparation of sections from paraffin-embedded tissues, the apoptotic tumour nuclei were detected using the TUNEL assay. Each

experiment included three or four slices for each treatment. For each slice, a total of 100–200 nuclei were counted.

Statistical evaluation

All data are reported as the mean ± the sample standard deviation (SD). Analysis of variance (ANOVA) was used to compare the tracer uptake, number of cells, apoptosis fraction and cell cycle distribution. An unpaired t test was used to compare the tumour growth rate, serum PSA value, apoptotic cell rate and PCNA-positive cell rate. Statistical significance was established at $p < 0.05$.

Results

Cellular uptake study

Figure 1a shows the number of 22Rv1 cells in each group. After 24-h incubation, there was no significant difference in the number of 22Rv1 cells among the standard medium and
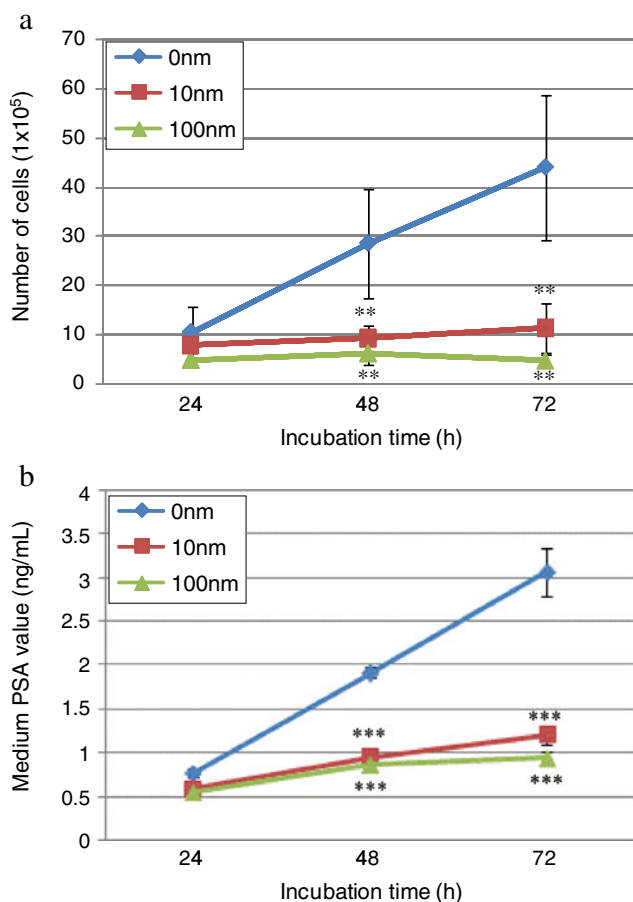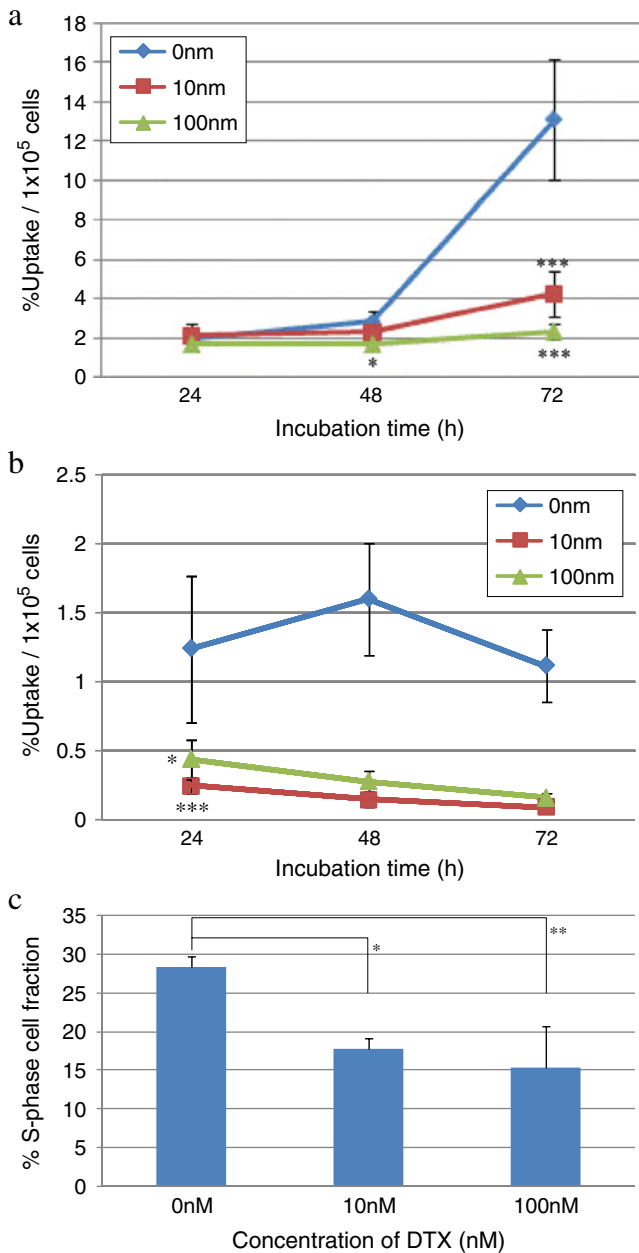
the media with 10 nM or 100 nM DTX (standard vs 10 nM DTX vs 100 nM DTX after 24-h incubation: $10.49 \pm 5.17 \times 10^5$ vs $8.00 \pm 2.87 \times 10^5$ vs $5.07 \pm 1.47 \times 10^5$). Following continuous incubation with the media containing DTX, the number of cells appeared to be lower than that in standard medium (standard vs 10 nM DTX or 100 nM DTX after 48-h incubation: $28.62 \pm 11.17 \times 10^5$ vs $9.33 \pm 2.57 \times 10^5$, $p < 0.01$ or $6.31 \pm 2.51 \times 10^5$, $p < 0.01$; after 72-h incubation: $44.09 \pm 14.89 \times 10^5$ vs $11.38 \pm 4.99 \times 10^5$, $p < 0.01$ or $4.89 \pm 0.99 \times 10^5$, $p < 0.01$). Figure 1b shows the PSA concentration in the media for each group. After 24-h incubation, there was a small difference in the PSA concentration among the three groups (standard vs 10 nM DTX vs 100 nM DTX at 24 h of incubation: 0.77 ± 0.05 ng/ml vs 0.580 ± 0.03 ng/ml vs 0.55 ± 0.04 ng/ml). Following continuous incubation with the media containing DTX, the PSA concentration appeared to be lower than in the standard media (standard vs 10 nM DTX or 100 nM DTX after 48-h incubation: 1.92 ± 0.06 ng/ml vs 0.95 ± 0.05 ng/ml, $p < 0.001$ or 0.87 ± 0.05 ng/ml, $p < 0.001$; after 72-h incubation: 3.07 ± 0.28 ng/ml vs 1.21 ± 0.11 ng/ml, $p < 0.001$ or 0.94 ± 0.07 ng/ml, $p < 0.001$). As shown in Fig. 2, after incubation in each medium, the FDG or FLT uptake in the cells was determined. There was no statistically significant difference in FDG uptake in the cells after 24-h incubation among the three groups. Following continuous incubation with the media containing DTX, the FDG uptake in the cells appeared to be lower than in the standard media (standard vs 10 nM DTX or 100 nM DTX after 48-h incubation: $2.81 \pm 0.53\%$ uptake/1×10^5 cells vs $2.29 \pm 0.36\%$ uptake/1×10^5 cells, not significant, or $1.66 \pm 0.22\%$ uptake/1×10^5 cells, $p < 0.05$; at 72-h incubation: $13.11 \pm 3.05\%$ uptake/1×10^5 cells vs $4.24 \pm 1.13\%$ uptake/1×10^5 cells, $p < 0.001$ or $2.31 \pm 0.42\%$ uptake/1×10^5 cells, $p < 0.001$) (Fig. 2a). On the other hand, there was a marked reduction of FLT uptake in the cells incubated in the medium containing DTX at 24 h of incubation ($1.24 \pm 0.53\%$ uptake/1×10^5 cells at standard medium, $0.24 \pm 0.04\%$ uptake/1×10^5 cells, $p < 0.001$ at 10 nM DTX, $0.44 \pm 0.14\%$ uptake/1×10^5 cells, $p < 0.05$ at 100 nM DTX) (Fig. 2b).

Flow cytometric study

After 24-h incubation in each medium, G_1, S and $G_2 + M$ fractions in the cells were determined. There was a marked reduction of % S-phase cell fraction of the cells incubated in the medium with DTX ($28.45 \pm 1.39\%$ at standard medium, $17.80 \pm 1.36\%$, $p < 0.05$ at 10 nM DTX; $15.33 \pm 5.31\%$, $p < 0.01$ at 100 nM DTX) (Fig. 2c).

MicroPET study

Tumour-bearing mice treated with DTX ($n=6$) or vehicle ($n=6$) for 2 weeks were scanned with the MicroPET

Fig. 1 The number of 22Rv1 cells among the standard medium and the media with 10 nM or 100 nM DTX (**p<0.01) (**a**) and the PSA concentration in three groups (***p<0.001) (**b**)

Fig. 2 FDG uptake in the cells among the three groups (*p<0.05, ***p<0.001) (**a**), FLT uptake in the cells (***p<0.001, *p<0.05) (**b**) and % S-phase cell fraction (*p<0.05, **p<0.01) (**c**)

scanner. The tumour size of each animal was also recorded. MicroPET images using FLT or FDG clearly demonstrated the tumours implanted in the left flank of the mice (Fig. 3). Static images at 2 h post-injection for FLT and 1 h post-injection for FDG were reconstructed, and ROIs were placed on the lumbar muscle and tumour using the same transverse images. Tracer uptake was compared in the same mice before and after 2-week DTX treatment using tumour to muscle ratios. Implanted tumours showed continuous growth during treatment (DTX vs vehicle: 1,459.6±1,015.0 mm^3 to 3,245.6± 2,096.7 mm^3 vs 916.8±738.5 mm^3 to 2,347.9±1,840.0 mm^3),

with no significant difference in the tumour growth rate between DTX- and vehicle-treated animals (DTX vs vehicle: 2.98±2.25 vs 2.51±1.46) (Fig. 4a). Serum PSA value was also compared before and after 2-week DTX treatment, showing no significant difference between two groups of animals (DTX vs vehicle: 3.90±3.41 vs 3.48±1.43) (Fig. 4b). The FLT study results are shown in Fig. 4c. The tumour to muscle ratios in the vehicle-treated mouse group were 5.34± 2.16 before treatment, and they were 3.79±1.28 after 2-week vehicle treatment, indicating a slight but not significant decrease in tracer uptake. On the other hand, the tumour to muscle ratios in the DTX-treated mice were 8.72±3.67 before treatment, and they were 2.82±0.53 after 2-week DTX treatment, indicating a significant decrease of FLT uptake after DTX treatment (p<0.05). The FDG study results are shown in Fig. 4d. There was no significant difference in FDG uptake in the implanted tumour between the baseline value and the value after DTX or vehicle treatment (baseline vs post-vehicle treatment: 3.32±1.34 vs 3.49±1.15; baseline vs post-DTX treatment: 4.22±1.28 vs 3.36±1.49).

Immunohistochemical examination of the 22Rv1 tumours

The results of the cellular proliferative study using PCNA staining are shown in Fig. 5a. The rates of cellular proliferation in the vehicle- and DTX-treated mice were 9.82±3.12% and 3.49±0.53% after 2 weeks of treatment, indicating a large decrease in the proliferative activity of the implanted tumour following DTX treatment (p<0.05). The results of an evaluation of the rate of apoptosis in the tumour using the TUNEL method are shown in Fig. 5b. The apoptotic indices in the vehicle- and DTX-treated mice were 0.78±0.12% and 0.67±0.12% after 2-week treatment, indicating that there was no difference in the apoptotic status between the two groups of mice.

Discussion

Monitoring the early therapeutic effects of chemotherapy, including DTX therapy, is crucial for patients with HRPC, because HRPC shows relatively rapid growth, leading to poor prognosis. Monitoring the anticancer effects is essential when deciding whether a certain kind of anti-cancer management should be maintained or should be changed for a better clinical outcome. For this purpose, tumour imaging including CT or MRI and evaluating serum PSA value are employed, which sometimes results in an insufficient evaluation of the early therapeutic effects. At this point, performing PET imaging of malignant tumours has a tremendous advantage because PET can be used to assess the metabolic status of cancer before it changes its anatomical form, which allows us to predict the reaction of
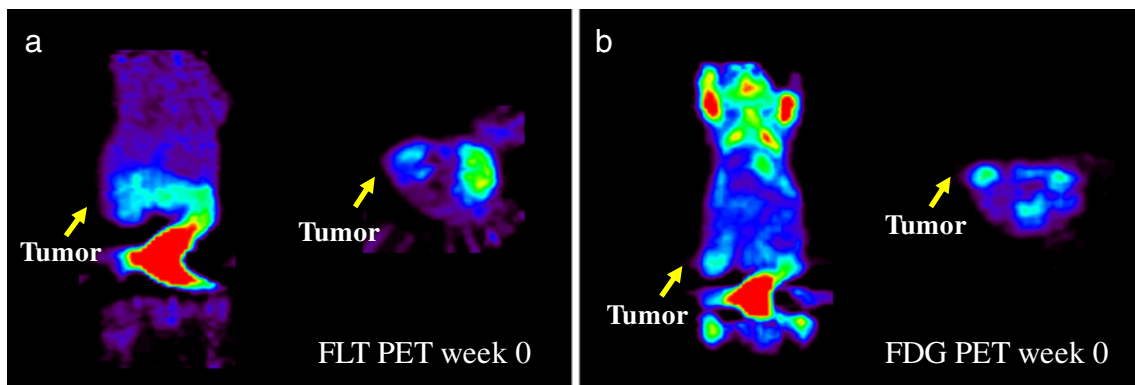
Fig. 3 MicroPET images of tumour implanted mice using FLT (**a**) and FDG (**b**)

a tumour to the chemotherapeutic agents as early as possible. Malignant tumours are characterized as tumours with a deregulated cell cycle progression resulting in rapid tumour growth. Enhanced proliferation of cancer cells demands an increased supply of DNA substrates, which are deoxynucleotides (dNTPs). Accordingly, analysis of DNA metabolism is as important a strategy as cancer imaging with PET. ^{11}C-Thymidine was the first radiopharmaceutical to assess cell proliferation for in vivo imaging

[21–24]. However, the short half-life of [11]C (20 min) with rapid degradation in vivo prevents ^{11}C-thymidine from seeing wide clinical use.

FLT is another thymidine analogue which has a longer half-life (110 min) because it is labelled with [18]F. According to a study by Shields et al., the FLT uptake in tissues depends on their proliferation activity [15]. Rasey et al. reported on the mechanisms of FLT uptake in the cell, showing that FLT uptake is positively correlated with cell
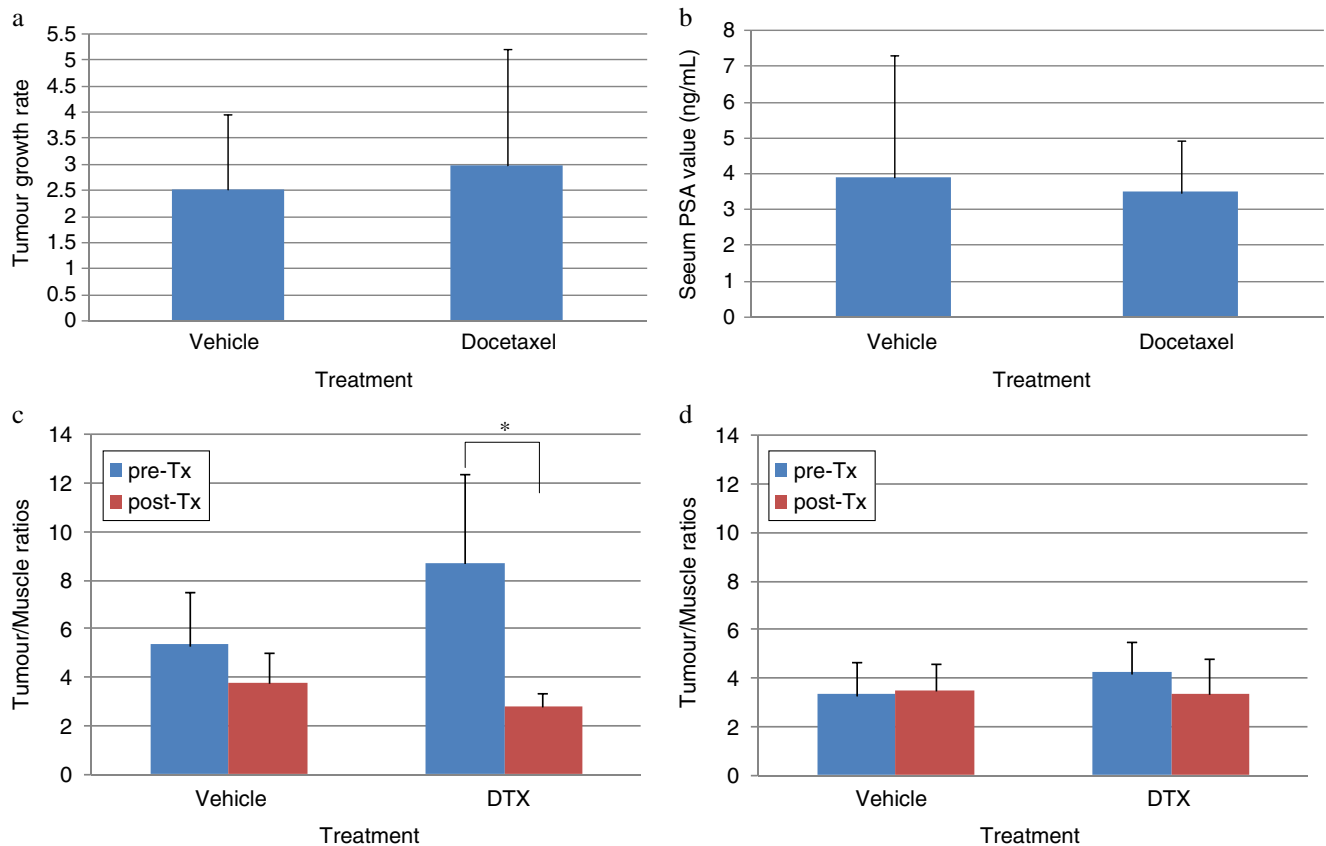
Fig. 4 Difference of tumour growth rate between the DTX- and vehicle-treated animals (**a**), difference of serum PSA value between the DTX- and vehicle-treated animals (**b**), difference of tumour to muscle ratios of FLT uptake between the two groups (*$p < 0.05$) (**c**) and difference of tumour to muscle ratios of FDG uptake between the two groups (**d**)
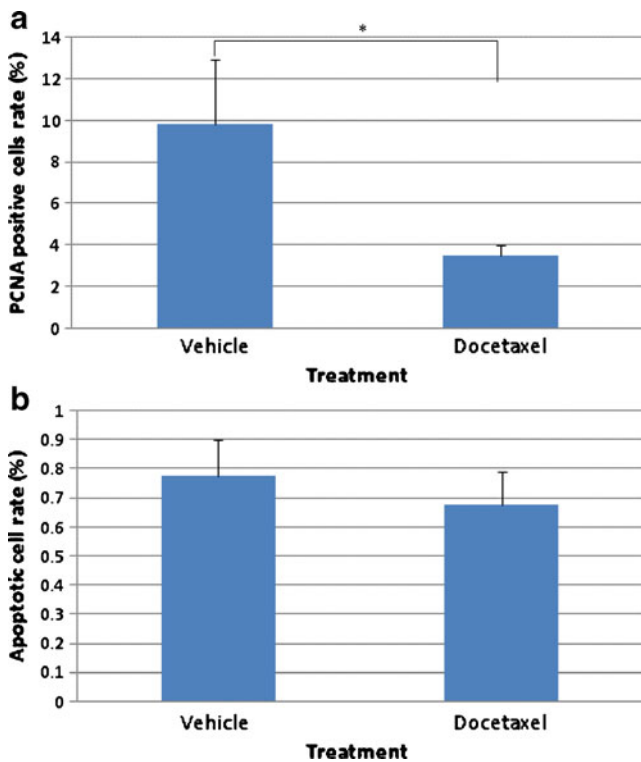
Fig. 5 The rates of cellular proliferation in the vehicle- and DTX-treated mice (*$p<0.05$) (a) and apoptotic indices in the vehicle- and DTX-treated mice (b)

growth and thymidine kinase 1 (TK1) activity and that inhibition of the cell cycle progression prevents FLT uptake and increased TK1 activity [25]. They concluded that FLT images reflect TK1 activity and the percentage of cells in S phase. These studies encouraged us to perform the current study to determine whether FLT is a useful tracer for monitoring the early therapeutic effects of DTX on HRPC in vitro and in vivo and also to determine whether FLT uptake in tumours correlates with actual proliferative activity after DTX therapy.

In our current study, DTX induced a significant inhibition of cell growth at 48 or 72 h post-treatment but not at 24 h in vitro. Production of PSA by the prostate cancer cells showed only a minimum inhibition at 24 h. These data indicate that 24-h DTX treatment is not long enough to induce an anticancer effect on tumour growth or the PSA production of 22Rv1 cells in vitro. Thus, longer treatment is needed to reveal such a difference. However, the flow cytometric study of the cells showed that there was a decrease in the S-phase cell fraction at 24 h of DTX treatment. This clearly shows that there is a chance to visualize the change in this DNA synthesis if we employ an adequate radiotracer to monitor the activity of DNA synthesis of the cells. We analysed two state-of-the-art PET tracers, FDG and FLT, for this purpose. As shown in this study, there was only a small change in FDG uptake in

the 22Rv1 cells at 24 h of DTX treatment, which showed that the cells in the early phase of cell cycle arrest may have normal glucose metabolism. This result agrees with the previous finding of an insignificant change in FDG uptake after chemotherapy [26]. On the other hand, there was a marked reduction of FLT uptake in the cells at 24 h of DTX treatment, whereas FDG uptake was still unchanged at this time point. This result clearly showed that FLT is a promising tracer for monitoring the early therapeutic effect of DTX on prostate cancer cells based on the changes of DNA synthesis. This result agrees with another study reporting a low uptake of FLT in cells treated with anticancer drugs [25].

In our animal study, we succeeded in visualizing implanted 22Rv1 tumours using microPET with FLT. We calculated the tumour growth rates of the implanted tumour by measuring the actual tumour size before and after 2-week treatment with vehicle or DTX and found that there was only a minimal difference in tumour size between before and after treatment with either vehicle or DTX. There was also no significant difference in the post-treatment change in the apoptotic index of the tumour between the two treatment groups. This indicated that 2-week DTX treatment may not be sufficient to induce anatomical changes of the implanted tumour even if animal CT is employed. Measuring serum PSA was not useful to monitor the anti-tumour effect of DTX at 2 weeks after treatment. These data indicate that 2-week treatment with DTX did not fully affect the tumour volume or PSA production in the tumour, and thus it seems to be difficult to observe the effects of DTX on HRPC using conventional monitoring methods. However, the immunohistochemical evaluation using the PCNA method demonstrated that there was a decrease in proliferative cells in the tumour implanted into the animals treated with DTX. This clearly showed that the evaluation of DNA synthesis in tumour cells can be an ideal strategy to determine the early anticancer effects of chemotherapeutic agents.

In the microPET study, a significant decrease of FLT uptake in tumours was demonstrated following 2-week DTX treatment, while there were no significant changes in the vehicle group. On the other hand, FDG uptake in tumours showed only minimal change in both groups. These microPET study results were well correlated with a change in the proliferation activity of the tumour determined by PCNA staining. This may indicate that 2-week DTX treatment of these animals influenced the TK1 activity of 22Rv1 cells, which has been well evaluated with FLT uptake. It is presumed that this change of TK1 activity comes into existence earlier than that of glucose metabolism, which can be evaluated with FDG uptake. Thus, FLT PET is superior to FDG for monitoring tumour proliferation activity after chemotherapy.

Our in vitro and in vivo studies both indicate that DTX treatment for a short period of time results in cell arrest of

22Rv1 prostate tumour cells without enhanced apoptotic cell death, and without reduction of both PSA production and glucose metabolism, while FLT PET appears to be useful as a tumour proliferation marker after DTX therapy. Ebenhan et al. recently reported the suitability of FDG, FLT, ^{18}F-methionine and ^{18}F-fluorocholine as noninvasive PET biomarkers for monitoring the response to chemotherapy [27]. In another study, they monitored the effects of patupilone, a novel cytotoxic compound that is a potent microtubule stabilizer [28], on FLT uptake in RIF-1 tumours and observed a significant decrease of tracer uptake after 24 h, which showed a strong negative correlation to apoptosis. Their results were consistent with our current study.

FLT has been well known for its high uptake to bone marrow. This feature of FLT may be helpful in evaluation of the effects of anticancer therapy on bone marrow for HRPC. According to the clinical study for oesophageal carcinoma by Yue et al., marked early reduction of proliferation in irradiated marrow was observed after only 2 Gy and complete absence of proliferation after 10 Gy [29]. They concluded that FLT PET can depict the effects of radiotherapy on bone marrow. Metastatic bone lesions are one of the common targets for DTX treatment for patients with HRPC. FLT PET could have a potential to evaluate the early anticancer effect of DTX on HRPC. Further in vivo and clinical investigations are needed to determine the role of FLT PET for bone marrow lesions. However, tracer uptake in bone marrow could be a limitation of FLT PET imaging for patients with HRPC when screening small osseous metastatic lesions. Detailed clinical study using FLT PET for patients with HRPC is needed.

One of the limitations of the current study was that many important parameters for androgen-independent prostate cancer such as serum androgen levels were neglected. A majority of the patients who have androgen-independent prostate cancer receiving chemotherapy including docetaxel also receive anti-androgen therapy, which lowers serum testosterone levels. This may also affect behaviour of FLT uptake in prostate cancer tissues. Further in vivo investigation seems to be necessary to clarify the role of FLT PET imaging for those patients receiving both DTX and AAT.

These results indicate that FLT is a promising tracer for monitoring the early therapeutic effects of DTX in patients with HRPC. Thus, FLT PET has potential for visualizing early-phase changes in the proliferation activity of HRPC after DTX treatment. Our data also suggest that FLT is superior to FDG in evaluation of the early therapeutic effect of DTX on HRPC.

Conclusion

These results indicate that ^{18}F-FLT is a promising tracer for monitoring the early therapeutic effects of DTX on HRPC.

Further clinical studies in humans will be needed to evaluate the possibility of using FLT PET to monitor the early therapeutic effects of DTX therapy.

Conflicts of interest None.

References

1. Jemal A, Siegel R, Ward E, Murray T, Xu J, Thun MJ. Cancer statistics, 2009. CA Cancer J Clin 2009;59:225–49.
2. Huggins C, Hodges CV. Studies on prostatic cancer: I. The effect of castration, of estrogen and of androgen injection on serum phosphatases in metastatic carcinoma of the prostate. Cancer Res 1941;1:293–7.
3. Eisenberger MA. Chemotherapy for prostate carcinoma. NCI Monogr 1988;7:151–63.
4. Petrylak DP, Tangen CM, Hussain MH, Lara PN Jr, Jones JA, Taplin ME, et al. Docetaxel and estramustine compared with mitoxantrone and prednisone for advanced refractory prostate cancer. N Engl J Med 2004;351:1513–20.
5. Oyama N, Kim J, Jones LA, Mercer NM, Engelbach JA, Sharp TL, et al. MicroPET assessment of androgenic control of glucose and acetate uptake in the rat prostate and a prostate cancer tumor model. Nucl Med Biol 2002;29:783–90.
6. Oyama N, Akino H, Suzuki Y, Kanamaru H, Ishida H, Tanase K, et al. FDG PET for evaluating the change of glucose metabolism in prostate cancer after androgen ablation. Nucl Med Commun 2001;22:963–9.
7. Kurdziel KA, Figg WD, Carrasquillo JA, Huebsch S, Whatley M, Sellers D, et al. Using positron emission tomography 2-deoxy-2-[18F]fluoro-D-glucose, 11CO, and 15O-water for monitoring androgen independent prostate cancer. Mol Imaging Biol 2003;5:86–93.
8. Effert PJ, Bares R, Handt S, Wolff JM, Büll D, Jakse G. Metabolic imaging of untreated prostate cancer by positron emission tomography with 18fluorine-labeled deoxyglucose. J Urol 1996;155:994–8.
9. Oyama N, Akino H, Suzuki Y, Kanamaru H, Sadato N, Yonekura Y, et al. The increased accumulation of [18F]fluorodeoxyglucose in untreated prostate cancer. Jpn J Clin Oncol 1999;29:623–9.
10. Hara T, Kosaka N, Kishi H. PET imaging of prostate cancer using carbon-11-choline. J Nucl Med 1998;39:990–5.
11. DeGrado TR, Baldwin SW, Wang S, Orr MD, Liao RP, Friedman HS, et al. Synthesis and evaluation of (18)F-labeled choline analogs as oncologic PET tracers. J Nucl Med 2001;42:1805–14.
12. Oyama N, Akino H, Kanamaru H, Suzuki Y, Muramoto S, Yonekura Y, et al. 11C-acetate PET imaging of prostate cancer. J Nucl Med 2002;43:181–6.

13. Yoshimoto M, Waki A, Yonekura Y, Sadato N, Murata T, Omata N, et al. Characterization of acetate metabolism in tumor cells in relation to cell proliferation: acetate metabolism in tumor cells. Nucl Med Biol 2001;28:117–22.

14. Yoshimoto M, Waki A, Obata A, Furukawa T, Yonekura Y, Fujibayashi Y. Radiolabeled choline as a proliferation marker: comparison with radiolabeled acetate. Nucl Med Biol 2004;31: 859–65.

15. Shields AF, Grierson JR, Dohmen BM, Machulla HJ, Stayanoff JC, Lawhorn-Crews JM, et al. Imaging proliferation in vivo with [F-18] FLT and positron emission tomography. Nat Med 1998;4:1334–6.

16. Buck AK, Schirrmeister H, Hetzel M, Von Der Heide M, Halter G, Glatting G, et al. 3-Deoxy-3-[18F]fluorothymidine-positron emission tomography for noninvasive assessment of proliferation in pulmonary nodules. Cancer Res 2002;62:3331–4.

17. Vesselle H, Grierson J, Muzi M, Pugsley JM, Schmidt RA, Rabinowitz P, et al. In vivo validation of 3'deoxy-3'-[(18)F] fluorothymidine ([(18)F]FLT) as a proliferation imaging tracer in humans: correlation of [(18)F]FLT uptake by positron emission tomography with Ki-67 immunohistochemistry and flow cytometry in human lung tumors. Clin Cancer Res 2002;8:3315–23.

18. Pio BS, Park CK, Pietras R, Hsueh WA, Satyamurthy N, Pegram MD, et al. Usefulness of 3'-[F-18]fluoro-3'-deoxythymidine with positron emission tomography in predicting breast cancer response to therapy. Mol Imaging Biol 2006;8:36–42.

19. Ponde DE, Oyama N, Welch MJ, McCarthy TJ. Synthesis of fluorothymidine ([18F]FLT) for radiotracer of tumors. Abstr Pap AM Chem S 2002;223:081-Nucl Part 2.

20. Tai YC, Chatziioannou A, Siegel S, Young J, Newport D, Goble RN, et al. Performance evaluation of the microPET P4: a PET system dedicated to animal imaging. Phys Med Biol 2001;46:1845–62.

21. Shields AF, Lim K, Grierson J, Link J, Krohn KA. Utilization of labeled thymidine in DNA synthesis: studies for PET. J Nucl Med 1990;31:337–42.

22. Goethals P, van Eijkeren M, Lodewyck W, Dams R. Measurement of [methyl-carbon-11]thymidine and its metabolites in head and neck tumors. J Nucl Med 1995;36:880–2.

23. Shields AF, Mankoff DA, Link JM, Graham MM, Eary JF, Kozawa SM, et al. Carbon-11-thymidine and FDG to measure therapy response. J Nucl Med 1998;39:1757–62.

24. Wells JM, Mankoff DA, Muzi M, O'Sullivan F, Eary JF, Spence AM, et al. Kinetic analysis of 2-[11C]thymidine PET imaging studies of malignant brain tumors: compartmental model investigation and mathematical analysis. Mol Imaging 2002;1:151–9.

25. Rasey JS, Grierson JR, Wiens LW, Kolb PD, Schwartz JL. Validation of FLT uptake as a measure of thymidine kinase-1 activity in A549 carcinoma cells. J Nucl Med 2002;43:1210–7.

26. Dittmann H, Dohmen BM, Kehlbach R, Bartusek G, Pritzkow M, Sarbia M, et al. Early changes in [18F]FLT uptake after chemotherapy: an experimental study. Eur J Nucl Med Mol Imaging 2002;29:1462–9.

27. Ebenhan T, Honer M, Ametamey SM, Schubiger PA, Becquet M, Ferretti S, et al. Comparison of [18F]-tracers in various experimental tumor models by PET imaging and identification of an early response biomarker for the novel microtubule stabilizer patupilone. Mol Imaging Biol 2009;11:308–21.

28. Altmann KH. Epothilone B and its analogs – a new family of anticancer agents. Mini Rev Med Chem 2003;3:149–58.

29. Yue J, Chen L, Cabrera AR, Sun X, Zhao S, Zheng F, et al. Measuring tumor cell proliferation with 18F-FLT PET during radiotherapy of esophageal squamous cell carcinoma: a pilot clinical study. J Nucl Med 2010;51:528–34.